Zero Lyapunov exponent in the vicinity of the saddle-node bifurcation point in the presence of noise

Alexander E. Hramov,* Alexey A. Koronovskii,† and Maria K. Kurovskaya‡
Faculty of Nonlinear Processes, Saratov State University, Astrakhanskaya, 83, Saratov, 410012, Russia
(Received 1 May 2008; revised manuscript received 30 July 2008; published 10 September 2008)

We consider a behavior of the zero Lyapunov exponent in the vicinity of the bifurcation point that occurs as the result of the interplay between dynamical mechanisms and random dynamics. We analytically deduce the laws for the dependence of this Lyapunov exponent on the control parameter both above and below the bifurcation point. The developed theory is applicable both to the systems with the random force and to the deterministic chaotic oscillators. We find an excellent agreement between the theoretical predictions and the data obtained by means of numerical calculations. We also discuss how the revealed regularities are expected to take place in other relevant physical circumstances.

DOI: 10.1103/PhysRevE.78.036212 PACS number(s): 05.45.Tp, 05.40.−a

INTRODUCTION

The Lyapunov exponents are known to be a very powerful tool for the analysis of the complex system dynamics. They are used widely to characterize the complex systems being the subjects of different fields of science, such as physics [1], molecular dynamics [2], astronomy [3], medicine [4], economy [5], etc.

One of the most advantageous applications of Lyapunov exponents is the use of them to detect the qualitative changes of the system behavior when control parameters of the system under study are varied. For example, the Lyapunov exponents are used to detect the transition from chaos to hyperchaos regime [6], to reveal the presence of hyperbolic attractor [1,7], to find the generalized synchronization [8,9] or noise induced synchronization [10–12] onset, etc.

The zero Lyapunov exponent stands out among the set of Lyapunov exponents characterizing the system dynamics. It corresponds to a perturbation along the trajectory in the phase space. Although this Lyapunov exponent may undergo alterations (e.g., it may become negative) when bifurcations take place, we use hereinafter the term "zero Lyapunov exponent" to refer exactly to this Lyapunov exponent both below and above the bifurcation point.

The zero Lyapunov exponent plays an important role in some relevant physical circumstances. For example, for the deterministic periodic oscillations the zero Lyapunov exponent is the largest one. Therefore, in such systems driven by the external signal (deterministic or stochastic) the largest conditional Lyapunov exponent (being the zero exponent in the autonomous case) may become negative, what would lead to a synchronization. Also, in the coupled chaotic oscillators the transition of one of the zero Lyapunov exponents to negative values is supposed to be closely connected with the onset of the phase synchronization regime (see [13,14] for detail). At the same time, it is known [15,16] that the points corresponding to the onset of the phase synchronization regime and to the transition of the zero Lyapunov exponent to the negative values do not coincide with each other and may differ sufficiently. Finally, the zero Lyapunov exponent may indicate the presence of a peculiar regime in the system dynamics, such as incomplete noise induced synchronization [17].

In this paper we study the behavior of the zero Lyapunov exponent in the vicinity of the saddle-node (tangential) bifurcation point in the presence of noise. Our studies of this subject are motivated by several important aspects. First, it is obvious, that the noise takes place both in experiments and numerical calculations. Although in some cases the presence of noise may be neglected, in the vicinity of the bifurcation point it may become crucial to the system dynamics. As a result, in the vicinity of the bifurcation boundary the system dynamics may be changed radically in comparison with the noiseless case. For example, the presence of noise is known to modify greatly the statistical characteristics of the intermittent behavior in the vicinity of the bifurcation point [18–21]. Therefore, it seems to be important both to recognize the manifestations of the noise influence on the significant quantities (such as Lyapunov exponents) characterizing the system dynamics and to understand particular features of the system behavior being revealed in the presence of noise.

Second, the subject of our consideration is connected tightly with such an intensively studied problem as phase synchronization [22,23]. Indeed, it is well known that for the periodically forced weakly nonlinear isochronous oscillator (in the case of a small frequency mismatch) the onset of the synchronous regime corresponds to the local saddle-node bifurcation (see, e.g., tutorial [24]). The very same scenario is observed in the case of phase synchronization of chaotic oscillators, although it is masked by the irregular dynamics [15,25]. Since in some cases the chaotic dynamics may be considered as a noise smeared periodic oscillations (see, e.g., [26]), the study of the regularities of the periodic system dynamics in the vicinity of the saddle-node bifurcation point in the presence of noise may reveal peculiar properties of the chaotic oscillator behavior close to the phase synchronization boundary.

The structure of the paper is the following. In Sec. I we develop the technique to estimate analytically the value of

*aeh@nonlin.sgu.ru
†alkor@nonlin.sgu.ru
‡mc@nonlin.sgu.ru

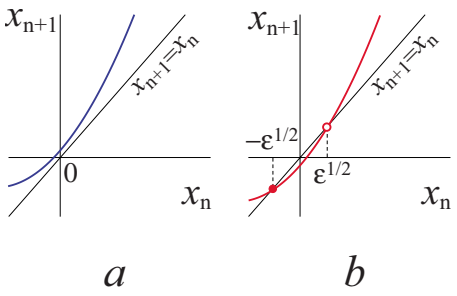

FIG. 1. (Color online) The iteration diagram for map (1) (a) $\varepsilon<0$ (subcritical region) and (b) $\varepsilon>0$ (supercritical region). The stable $x_s=-\varepsilon^{1/2}$ and unstable $x_u=\varepsilon^{1/2}$ fixed points of (1) are shown by ● and ○, respectively

the zero Lyapunov exponent both below and above the saddle-node bifurcation point in the presence of noise. We show that in the subcritical region even small noise turn the Lyapunov exponent into the negative values. The consequences of such alteration in the Lyapunov exponent behavior are discussed later, in the next sections. In Secs. II and III we show numerically that our theoretical predictions are observed in the different nonlinear systems, including coupled chaotic oscillators near the boundary of the phase synchronization in the case of small detuning of the natural frequencies. In Sec. II the analytical equations obtained in Sec. I are compared with the results of numerical calculations of the dynamics of the model systems (such as circle map and Van der Pol oscillator driven by the external harmonic signal) in the presence of white δ-correlated noise. Next, in Sec. III we consider the dependence of the zero Lyapunov exponent on the coupling strength for two coupled Rössler oscillators and discuss the particularities of the system dynamics corresponding to the negativeness of the zero Lyapunov exponent. The final conclusions are given at the end of the paper.

I. ZERO LYAPUNOV EXPONENT IN THE VICINITY OF BIFURCATION POINT: ANALYTICAL APPROACH

Let us estimate the zero Lyapunov exponent in the vicinity of the saddle-node bifurcation in the presence of noise. In the noiseless case the standard model of the saddle-node bifurcation is the one-parameter quadratic map

$$x_{n+1}=F(x_n)=x_n+x_n^2-\varepsilon, \tag{1}$$

where ε is a control parameter. The value of $\varepsilon_c=0$ corresponds to the saddle-node (tangential) bifurcation when the stable and unstable points $x_{u,s}=\pm\varepsilon^{1/2}$ touch each other in $x=0$ and disappear.

Above the critical parameter value (i.e., for $\varepsilon>\varepsilon_c$), the stable fixed point $x_s=-\varepsilon^{1/2}$ is observed and one can obtain easily that the Lyapunov exponent being the main subject of our study is $\lambda_0=\ln|1-2\sqrt{\varepsilon}|$ in the supercritical region. Below ε_c, in the subcritical region, a narrow corridor between the function $F(x)$ and the bisector $x_{n+1}=x_n$ exists, so that the point representing the state of the map (1) moves along this passage (Fig. 1 and, finally, leaves it. Due to the presence of the higher-order terms neglected in quadratic map (1) in the dissipative dynamical systems the reinjection process may take place when the phase trajectory arrives back to the onset of the corridor, after that the process is repeated iteratively. This phenomenon is well known as type-I intermittency [27,28], with Eq. (1) being also used as a classical model of this type of the intermittent behavior taking place in the vicinity of the saddle-node bifurcation.

The motion of the representation point along the corridor is considered as a laminar phase of the type-I intermittency. Alternatively, the reinjection process that is supposed to take place returns the phase trajectory to the onset of the corridor and is regarded as a turbulent phase. During the laminar phase two near trajectories converge together for $x<0$ and diverge from each other for $x>0$. Due to the symmetry of the corridor between the function $F(x)$ and the bisector $x_{n+1}=x_n$ one can expect that the value of the Lyapunov exponent is equal to zero in this case. This conclusion agrees well with the fact that the dynamics of system (1) in the subcritical region corresponds to the asynchronous oscillations of the periodically forced weakly nonlinear isochronous oscillator at the onset of the synchronous regime, where the required Lyapunov exponent λ_0 is known to be equal to zero. Therefore, in the case without noise the zero Lyapunov exponent depends on the control parameter ε as

$$\lambda_0(\varepsilon)=\begin{cases}0 & \text{if } \varepsilon<0,\\ \ln|1-2\sqrt{\varepsilon}| & \text{if } \varepsilon\geqslant 0.\end{cases} \tag{2}$$

Obviously, the influence of noise may alter these relations. To estimate the value of the required zero Lyapunov exponent in the presence of noise, we consider the same quadratic map (1) with the addition of a stochastic term ξ_n,

$$x_{n+1}=f(x_n)=x_n+x_n^2-\varepsilon+\xi_n, \tag{3}$$

where ξ_n is supposed to be a δ-correlated Gaussian white noise [$\langle\xi_n\rangle=0$, $\langle\xi_n\xi_m\rangle=D\delta(n-m)$] [43,44].

The Lyapunov exponent Λ_0 of system (3) may be found in the form

$$\Lambda_0(\varepsilon)=\lim_{n\to\infty}\frac{1}{n}\sum_{i=0}^{n-1}\ln|f'(x_i)|, \tag{4}$$

where x_n is the time series generated by the system (3).

Having supposed the ergodicity of the considered process and the presence of the reinjection one can substitute the time averaging with the ensemble one,

$$\Lambda_0(\varepsilon)=\int_{-\infty}^{+\infty}\rho_i(x)\ln|f'(x)|dx, \tag{5}$$

where $\rho_i(x)$ is the invariant probability density of x variable.

To obtain the invariant probability density $\rho_i(x)$ we suppose that (i) the value of $|\varepsilon|$ is rather small and (ii) the value of x changes per one iteration insufficiently. Hence, we can consider $(x_{n+1}-x_n)$ as the time derivative $\dot{x}$ and undergo from the system with discrete time (3) to the flow system, in the same way as in the case of the classical theory of the type-I intermittency [29]. Since the stochastic term is present in (3) we must examine the stochastic differential equation

$$dX = (X^2 - \varepsilon)dt + dW, \tag{6}$$

where $X(t)$ is a stochastic process, $W(t)$ is a one-dimensional Wiener process.

The stochastic differential equation (6) is equivalent to the Fokker-Planck equation

$$\frac{\partial \rho_X(x,t)}{\partial t} = -\frac{\partial}{\partial x}[(x^2 - \varepsilon)\rho_X(x,t)] + \frac{D}{2}\frac{\partial^2 \rho_X(x,t)}{\partial x^2} \tag{7}$$

for the probability density $\rho_X(x,t)$ of the stochastic process $X(t)$. To reduce the number of the control parameters the normalization $z = x/\sqrt{|\varepsilon|}$, $\tau = t\sqrt{|\varepsilon|}$ may be used, after which Eq. (7) may be rewritten in the form

$$\frac{\partial \rho_Z(z,\tau)}{\partial \tau} = -\frac{\partial}{\partial z}[(z^2 \pm 1)\rho_Z(z,\tau)] + \frac{D^*}{2}\frac{\partial^2 \rho_Z(z,\tau)}{\partial z^2}, \tag{8}$$

where the sign "plus" should be taken for the subcritical region $\varepsilon < 0$ and "minus" for the supercritical one $\varepsilon > 0$, $D^* = D|\varepsilon|^{-3/2}$, $\rho_Z(z,\tau) = \sqrt{|\varepsilon|}\rho_X(z|\varepsilon|^{1/2}, \tau|\varepsilon|^{-1/2})$.

Unfortunately, we cannot obtain the universal relation defining the zero Lyapunov exponent both in the subcritical and supercritical regions simultaneously, since the character of the system behavior is radically different for the negative and positive values of the control parameter ε. Hence, let us consider the dynamics of system (3)) in the subcritical and supercritical regions separately to deduce the analytical approximations of the zero Lyapunov exponent in the vicinity of the bifurcation point in the presence of noise.

A. Subcritical region, $\varepsilon < 0$

Let $\rho_I(z)$ be the stationary probability density being the solution of the Fokker-Planck equation (8) corresponding to stochastic map (3) behavior in the subcritical region. Since $\rho_I(z)$ does not depend on time, it satisfies the condition

$$\frac{D^*}{2}\rho_I'(z) - [(z^2 + 1)\rho_I(z)] = c, \tag{9}$$

where c is constant.

We find the stationary probability density $\rho_I(z)$ in the form of the power series expansion in the small parameter D^*,

$$\rho_I(z) = \rho_0(z) + D^*\rho_1(z) + O(D^{*2}), \tag{10}$$

with $\rho_I(z)$ satisfying the normalization condition

$$\int_{-\infty}^{+\infty} \rho_I(z)dz = 1. \tag{11}$$

Having restricted ourselves to the first term of series expansion (10), we obtain

$$\rho_I(z) = \frac{1}{\pi(z^2 + 1)} - D^*\frac{z}{\pi(z^2 + 1)^3} + O(D^{*2}). \tag{12}$$

Taking into account Eq. (3), Eq. (5) and the relationship between variables z and x, the zero Lyapunov exponent Λ_0 may be estimated as

$$\Lambda_0(\varepsilon) = \int_{-\infty}^{+\infty} \rho_I(z)\ln|1 + 2\sqrt{(-\varepsilon)}z|dz. \tag{13}$$

Since we consider the system dynamics in the vicinity of the bifurcation point (i.e., close to $\varepsilon_c = 0$), the value of the control parameter ε is assumed to be sufficiently small, whereas $\rho_I(z)$ decreases rapidly when $|z|$ grows. Therefore, we can expand $\ln|1 + 2\sqrt{(-\varepsilon)}z|$ in a series and use only the first term $2\sqrt{(-\varepsilon)}z$ of it. Then,

$$\begin{aligned}
\Lambda_0(\varepsilon) &\simeq 2\sqrt{(-\varepsilon)}\int_{-\infty}^{+\infty} z\rho_I(z)dz \\
&= 2\sqrt{(-\varepsilon)}\int_{-\infty}^{+\infty} z\rho_0(z)dz + D^*2\sqrt{(-\varepsilon)}\int_{-\infty}^{+\infty} z\rho_1(z)dz \\
&= \frac{\sqrt{(-\varepsilon)}}{\pi}\ln(1 + z^2)\Big|_{-\infty}^{+\infty} \\
&\quad - D^*\sqrt{(-\varepsilon)}\frac{\dfrac{z(z^2 - 1)}{(1 + z^2)^2} + \arctan(z)}{4\pi}\Bigg|_{-\infty}^{+\infty} \\
&= -\frac{D^*\sqrt{(-\varepsilon)}}{4} = -\frac{D}{4|\varepsilon|}.
\end{aligned} \tag{14}$$

As it follows from Eq. (14), in the subcritical region the Lyapunov exponent Λ_0 under study is really equal to zero if there is no noise in the system (i.e., if $D = 0$), whereas even small noise turns the zero Lyapunov exponent Λ_0 into the negative values. The consequence of this alteration in the zero Lyapunov exponent behavior will be discussed below in Sec. III.

Note also, that Eq. (14) is valid only for the negative values of the control parameter ε and cannot be used in the supercritical region. Moreover, in the negative area this approximation is applicable only in the certain region of the values of the control parameter ε. In particular, although it follows from Eq. (14) that the zero Lyapunov exponent tends to zero when $\varepsilon \to -\infty$, this deduction cannot be used, since our theory has been developed under the assumption of the smallness of the value of $|\varepsilon|$ only (in other words, we suppose that $|\varepsilon| \ll 1$). Indeed, if the value of $|\varepsilon|$ is not small, the difference $(x_{n+1} - x_n)$ cannot be considered as the time derivative $\dot{x}$ and, therefore, one cannot undergo from the system with discrete time (3) to the stochastic differential equation (6). Similarly, our theoretical prediction (14) is not applicable for the extremely small negative values of the control parameter ε (i.e., for $\varepsilon \to -0$), that is caused by the major transformation of the system behavior when the control parameter ε undergoes from the subcritical region to the supercritical one. Obviously, when the type of the behavior is changed radically, our assumptions made in the subcritical region for deriving Eq. (14) stops being correct and, therefore, Eq. (14) becomes inapplicable to the zero Lyapunov exponent estimation. In other words, expression (14) differs from the true value of the zero Lyapunov exponent in the limit $\varepsilon \to -0$ and diverges at $\varepsilon_c = 0$.

Let us estimate the range of the control parameter values in the subcritical region where our theoretical prediction should be valid. As it was discussed above, the first constraint is $|\varepsilon| \ll 1$. The second one can be obtained formally from Eq. (10) which converges when D^* is small. If the value of D^* stops being small, series (10) diverges. Therefore, one can expect, that the obtained relation (14) is correct when $D^* \ll 1$, and $D \ll |\varepsilon|^{3/2}$, correspondingly. Thus, for the subcritical region the obtained theoretical prediction is valid in the range

$$D^{2/3} \ll |\varepsilon| \ll 1. \tag{15}$$

B. Supercritical region, $\varepsilon > 0$

Let us estimate the zero Lyapunov exponent Λ_0 in the region of the positive values of the control parameter ε. As it was mentioned above, if the intensity of noise D is equal to zero, in the supercritical region the zero Lyapunov exponent is negative and it is determined by Eq. (2).

Contrary to the subcritical region, the influence of noise does not happen to change the value of the zero Lyapunov exponent sufficiently. The stationary probability density $\rho_I(z)$ for the positive values of the control parameter ε was reported in [20], where it was deduced as a solution of the Foker-Planck equation (8). Taking into consideration the reinjection process, it may be written in the form

$$\rho_I(z) = C\frac{2}{D^*}\exp\left[-\frac{2}{D^*}\left(z - \frac{z^3}{3}\right)\right], \tag{16}$$

where C is the normalization constant, providing (11). The obtained probability density $\rho_I(z)$ is localized in the small interval of the values of z variables, its maximum is located in the point $z_0 = -1$, with Eq. (16) being applicable only for $z < +1$ (see [20] for detail). For the further analysis it is appropriate to rewrite Eq. (16) in the form

$$\rho_I(\eta) = C\frac{2}{D^*}\exp\left(\frac{4}{3D^*} - \frac{2}{D^*}\eta^2 + \frac{2}{3D^*}\eta^3\right), \tag{17}$$

where $\eta = z + 1$, to consider the probability density in the vicinity of the maximum point. In the region where $|\eta| \ll 1$ the cubic term of Eq. (17) may be neglected and, therefore, one can estimate the probability density there as

$$\rho_I(\eta) \simeq C\frac{2}{D^*}\exp\left(\frac{4}{3D^*}\right)\exp\left(-\frac{2}{D^*}\eta^2\right). \tag{18}$$

Based on the asymptotic approximation of Dirac δ function

$$\delta(\eta) = \lim_{\alpha\to\infty}\frac{\alpha}{\sqrt{\pi}}\exp(-\alpha^2\eta^2) \tag{19}$$

and normalization condition (11), we conclude that for the small values of D^* the stationary probability density $\rho_I(z)$ may be considered as an approximation of δ function, i.e.,

$$\rho_I(z) \simeq \delta(z+1). \tag{20}$$

Then, the zero Lyapunov exponent in the supercritical region may be estimated as

$$\Lambda_0(\varepsilon) \simeq \int_{-\infty}^{+\infty}\delta(z+1)\ln|1 + 2\sqrt{\varepsilon}z|dz = \ln|1 - 2\sqrt{\varepsilon}|. \tag{21}$$

Thus, above the bifurcation point the noise does not effect practically on the zero Lyapunov exponent, and its value Λ_0 coincides with the value of the corresponding Lyapunov exponent λ_0 characterizing the dynamics of system without noise.

Again, as for the subcritical region, expression (21) for the zero Lyapunov exponent is not applicable for the extremely small positive values of the control parameter ε (i.e., $\varepsilon \to +0$). Let us obtain the boundary of the ε values where our theoretical prediction (21) is applicable. For approximation (20) to be correct the stationary probability density $\rho_I(\eta)$ must decrease greatly in the range $|\eta| \ll 1$ that is possible only if the value of D^* is small sufficiently. In this case the D^* quantity performs a role of the variance: The more the value of D^* is, the more the width of the stationary probability density $\rho_I(\eta)$ becomes. When the value of D^* stops being small, the range where $\rho_I(\eta)$ decreases greatly does not satisfy the condition $|\eta| \ll 1$. As a result, the cubic term of Eq. (17) cannot be neglected and, therefore, approximation (20) of the stationary probability density $\rho_I(z)$ by the δ function becomes incorrect. Thus, our assumptions made to deduce Eq. (21) are correct if and only if $D^* \ll 1$ or $D \ll \varepsilon^{3/2}$. Therefore, the theoretical prediction of the zero Lyapunov exponent value in the supercritical region is applicable for

$$\varepsilon \gg D^{2/3}. \tag{22}$$

Note also, that since the obtained solutions (14) and (21) diverge from the true value of the zero Lyapunov exponent in the limit $\varepsilon \to 0$, they are not joined together in the point $\varepsilon = 0$.

II. ZERO LYAPUNOV EXPONENT IN THE VICINITY OF BIFURCATION POINT: NUMERICAL CALCULATIONS OF BEHAVIOR OF MODEL SYSTEMS

Let us consider now the behavior of two model systems (with a stochastic force added) in the vicinity of the saddle-node bifurcation point for the analytical results obtained in the preceding section to be verified. As such test systems we have selected (i) the circle map and (ii) driven Van der Pol oscillator. The first of them is a dynamical system with discrete time, being the simple model of synchronization phenomena, while the second one is a system with the continuous time. Both the circle map and Van der Pol oscillator are used widely in the nonlinear theory as the simple model systems.

A. Circle map

We start studying the zero Lyapunov exponent behavior considering the circle map

$$x_{n+1} = x_n + 2\Omega(1 - \cos x_n) - \varepsilon + \xi_n, \quad \mod 2\pi \tag{23}$$

on the interval $x \in [-\pi, \pi)$, where ε is the control parameter, $\Omega = 0.1$, ξ_n is supposed to be a δ correlated Gaussian white

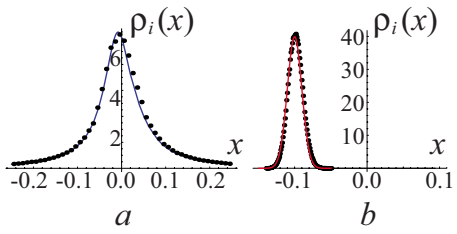

FIG. 2. (Color online) The stationary probability density $\rho_i(x)$ of x variable. The theoretical dependencies of the probability density on the coordinate are shown by the red solid lines, the numerically calculated data for (23) are shown by points (●). The control parameter values are $\Omega=0.1$, $D=4\times10^{-6}$. (a) Subcritical region, $\varepsilon=-2\times10^{-4}$. (b) Supercritical region, $\varepsilon=10^{-3}$

noise $[\langle\xi_n\rangle=0, \langle\xi_n\xi_m\rangle=D\delta(n-m)]$. If the intensity of noise D is equal to zero, the saddle-node bifurcation is observed in (23) for $\varepsilon=\varepsilon_c=0$, when the stable and unstable fixed points annihilate in $x=0$. Obviously, in the vicinity of the bifurcation point the evolution of system (23) may be described with the help of the quadratic map

$$x_{n+1}=x_n+\Omega x_n^2-\varepsilon+\xi_n, \tag{24}$$

allowing an easy comparison between theoretical predictions given in the preceding section and results of direct numerical calculations of map (23) dynamics.

The approximations of the probability density $\rho_i(x)$ for circle map (23) and the zero Lyapunov exponent $\Lambda_0(\varepsilon)$ take the forms of

$$\rho_i(x)\simeq\begin{cases}\dfrac{\sqrt{\Omega\varepsilon}}{\pi(\varepsilon+\Omega x^2)}-D\dfrac{\Omega\sqrt{\Omega\varepsilon}x}{\pi(\varepsilon+\Omega x^2)^3}, & \varepsilon<0,\\ \dfrac{\sqrt{2}(\Omega\varepsilon)^{1/4}}{\sqrt{\pi D}}\exp\left[-\dfrac{2\sqrt{\varepsilon}}{D\Omega}\left(x+\sqrt{\dfrac{\varepsilon}{\Omega}}\right)^2\right], & \varepsilon>0,\end{cases} \tag{25}$$

and

$$\Lambda_0(\varepsilon)\simeq\begin{cases}-\dfrac{D\Omega}{4|\varepsilon|}, & \varepsilon<0,\\ \ln|1-2\sqrt{\Omega\varepsilon}|, & \varepsilon>0,\end{cases} \tag{26}$$

respectively.

The stationary probability densities $\rho_i(x)$ of x variable are shown in Fig. 2 for subcritical and supercritical regions of the control parameter. The solid curves correspond to the analytical predictions, while the points represent data obtained by direct numerical simulations of (23). One can see the excellent agreement between the theoretical curves and numerically calculated points both for $\varepsilon<0$ and $\varepsilon>0$.

As it follows from Eq. (25), if the intensity of noise D is equal to zero, in the subcritical region the form of the probability density $\rho_i(x)$ is symmetrical with maximum being in $x=0$. The symmetry of the probability density results in the zero value of the Lyapunov exponent λ_0. The noise added breaks the symmetry and shifts the extremum point towards negative values of x coordinate, and, as a result, the considered Lyapunov exponent Λ_0 becomes negative. As far as the supercritical region is concerned, the stationary probability density $\rho_i(x)$ is very close to the asymptotic approximation by Dirac δ function (19) taken in the form of the normal distribution (25).

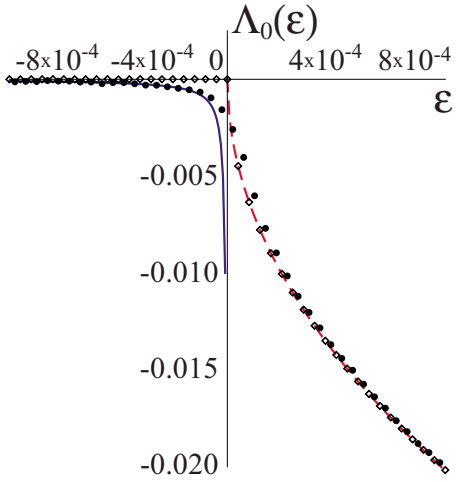

FIG. 3. (Color online) The dependence of the zero Lyapunov exponent Λ_0 on the control parameter ε in the vicinity of the saddle-node bifurcation point for the circle map (23). The control parameter value is $\Omega=0.1$. The numerically calculated data are shown by points ◇ ($D=0$) and ● ($D=4\times10^{-6}$). The analytical expressions for the zero Lyapunov exponent (26) are shown by a solid line in the subcritical region and by a dashed line in the supercritical range of control parameter values.

Figure 3 shows the dependence of the zero Lyapunov exponent (●) on the control parameter ε as well as its approximations (26) both in the subcritical and supercritical regions. The zero Lyapunov exponent in the case without noise (◇) is also shown in Fig. 3. Again, there is an excellent coincidence between theoretical predictions and numerically calculated values, except for the very tiny range of the extremely small values of the control parameter ε, where (in the full agreement with the theory given in Sec. I) the analytical formulas diverge from the true values of Lyapunov exponent.

Let us now compare the results of the numerical simulations performed for the different values of the noise amplitude D and control parameter ε with the theoretical predictions (26) to verify the conditions (15) and (22). The dependencies of the zero Lyapunov exponent Λ_0 on the control parameter ε in the subcritical region are shown in Fig. 4(a) in log-log scale for three different values of the noise intensity $D_1=10^{-6}$ (○), $D_2=4\times10^{-6}$ (●) and $D_3=9\times10^{-6}$ (◇), curves 1, 2, and 3, respectively. The theoretical predictions are shown by lines, whereas the numerically calculated data are shown by points. One can see that the numerically obtained results agree very well with the theoretical approximations for all noise intensities. At the same time, for the extremely small values of $|\varepsilon|$ the points obtained by numerical calculations deviate from the straight lines prescribed by the theory, with this deviation also agreeing very well with (15). Indeed, one can expect, that the noticeable deviation should be observed for $|\varepsilon|\approx D^{2/3}$. Having substituted $|\varepsilon|^{3/2}$ for D in the first line of (26), we obtain the expression

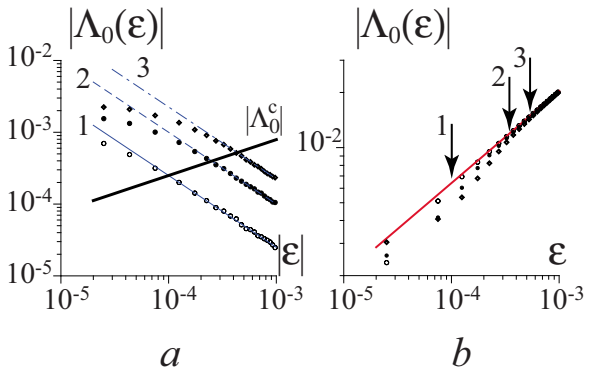

FIG. 4. (Color online) The dependencies of the absolute value of the zero Lyapunov exponent Λ_0 on the control parameter ε in the subcritical (a) and supercritical (b) regions shown in log-log scale for three different values of the noise intensity. The control parameter value is $\Omega=0.1$. The numerically calculated data are shown by points (symbols "○" for $D_1=10^{-6}$, "●" for $D_2=4\times10^{-6}$ and "◇" for $D_3=9\times10^{-6}$), whereas the analytical expressions for the zero Lyapunov exponent (26) are shown by lines (in the subcritical region curves 1, 2, and 3 for $D_1=10^{-6}$, $D_2=4\times10^{-6}$, and $D_3=9\times10^{-6}$, respectively). The critical points where the analytical approximation (26) becomes inapplicable are shown by the solid line $|\Lambda_0^c|$ in the subcritical region and by arrows 1–3 in the supercritical one (see text for details).

$$\Lambda_0^c(\varepsilon) = -\sqrt{|\varepsilon|}/4 \tag{27}$$

for the critical values of the zero Lyapunov exponent corresponding to the points where the analytical approximation (26) becomes inapplicable. The line determined by Eq. (27) is also shown in Fig. 4(a). One can expect, that below this line, where $D<|\varepsilon|$, the theoretical prediction (26) should agree well with the numerically calculated data, whereas above this line ($D>|\varepsilon|$) the true values of the zero Lyapunov exponent should differ from the theoretical approximations. It is easy to see, that it is this situation that takes place in Fig. 4(a): For all values of the noise intensity the numerically obtained points start deviating from the theoretical lines in the points prescribed by the critical curve Λ_0^c.

The analogous comparison between the theoretical predictions and numerically obtained data for the supercritical region is given in Fig. 4(b). Since the estimated values of the zero Lyapunov exponent in the supercritical region do not depend on the noise intensity, the points calculated numerically for the different values of D parameter (symbols "○" for $D_1=10^{-6}$, "●" for $D_2=4\times10^{-6}$ and "◇" for $D_3=9\times10^{-6}$) are approximated by only one line. At the same time, the values of ε where the points obtained numerically deviate from the theoretical curve (26) depend noticeably on the noise intensity D. Based on the condition (22) one can expect that for the noise intensity D this deviation should be observed at $\varepsilon_c=D^{2/3}$. These critical values of ε parameter are shown in Fig. 4(b) by arrows ($\varepsilon_{c1}=10^{-4}$ for $D_1=10^{-6}$, arrow 1; $\varepsilon_{c2}\approx2.5\times10^{-4}$ for $D_2=4\times10^{-6}$, arrow 2 and $\varepsilon_{c3}\approx4.3\times10^{-4}$ for $D_3=9\times10^{-6}$, arrow 3). Again, as well as in the case of the subcritical region, there is an excellent agreement between the results of the numerical calculations and developed theory.

B. Van der Pol oscillator

As it was mentioned above the behavior of the zero Lyapunov exponent is related to the synchronization phenomenon. Therefore, as the second model we consider a Van der Pol oscillator

$$\ddot{x} - (\mu - x^2)\dot{x} + x = A\sin(\omega_e t) + \xi(t) \tag{28}$$

driven by an external harmonic signal with the amplitude A and frequency ω_e, with an added stochastic term $\xi(t)$, where $\xi(t)$ is a δ-correlated Gaussian white noise [$\langle\xi(t)\rangle=0$, $\langle\xi(t)\xi(\tau)\rangle=D\delta(t-\tau)$].

The values of the control parameters are selected to be $\mu=0.1$, $\omega_e=0.98$. For these control parameters and for $D=0$, the dynamics of the driven Van der Pol oscillator becomes synchronized when $A=A_c=0.0238$. To integrate Eq. (28) the one-step Euler method has been used with a time step $h=5\times10^{-4}$.

It is well known that the saddle-node bifurcation is observed for the periodically forced weakly nonlinear isochronous oscillator (in the case of a small frequency mismatch) at the onset of the synchronous regime. Indeed, the complex amplitude method may be used to find the solution describing the oscillator behavior in the form

$$u(t) = \mathrm{Re}\, a(t)e^{i\omega t}. \tag{29}$$

For the complex amplitude $a(t)$ one obtains averaged (truncated) equation

$$\dot{a} = -i\nu a + a - |a|^2 a - ik, \tag{30}$$

where ν is the frequency mismatch, and k is the (renormalized) amplitude of the external force. For the small ν and large k the stable solution

$$a(t) = Ae^{i\phi} = \mathrm{const} \tag{31}$$

corresponds to the synchronous regime, with the synchronization destruction corresponding to the local saddle-node bifurcation associated with the global bifurcation of the limit cycle birth [24]. In this case, below the bifurcation point (the subcritical values of the amplitude of the external force) the largest conditional Lyapunov exponent is equal to zero, while in the supercritical region of the k-parameter values the largest conditional Lyapunov exponent becomes negative that manifests the presence of the synchronous dynamics. It is the Lyapunov exponent λ_0 taking the zero value in the subcritical region of the control parameter below the saddle-node bifurcation point (i.e., the zero Lyapunov exponent) that is the main subject of interest of the present study.

The influence of the additive noise modifies the oscillator behavior in the same way as in the case of the circle map considered. Since theoretical expressions (14) and (21) have been obtained in Sec. I for the model system with discrete time, they should be adapted to the flow systems. Generally, the dependence of the zero Lyapunov exponent on the control parameter $(\varepsilon-\varepsilon_c)$ may be written as

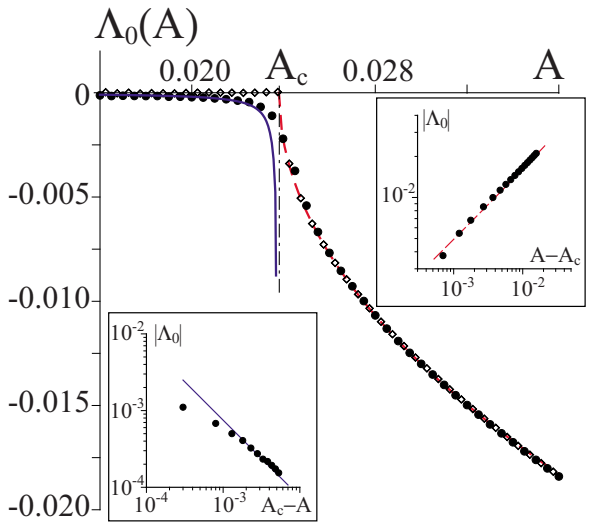

FIG. 5. (Color online) The dependence of the zero Lyapunov exponent Λ_0 on the control parameter A in the vicinity of the saddle-node bifurcation point for the Van der Pol oscillator (28). The bifurcation point $A_c=0.0238$ is shown by the dotted line. The numerically calculated data are shown by points ◇ ($D=0$) and ● ($D=1.0$). The analytical expressions for the zero Lyapunov exponent are shown by a solid line in the subcritical region and by a dashed line in the supercritical range of control parameter values. In the frames the same points obtained numerically ($D=1.0$) as well as function (32) are shown in log-log scale both for the subcritical and supercritical regions of the A parameter.

$$\Lambda_0(\varepsilon) \simeq \begin{cases} -\dfrac{a_1}{|\varepsilon-\varepsilon_c|}, & \varepsilon < \varepsilon_c, \\ f \ln|1-a_2\sqrt{\varepsilon-\varepsilon_c}|, & \varepsilon > \varepsilon_c, \end{cases} \tag{32}$$

where f is the frequency of the external signal, a_1 and a_2 are constants determined by the system under study; ε, control parameter; ε_c, bifurcation point.

For Van der Pol oscillator (28) the amplitude A of the external signal is considered as a control parameter. The dependence of the zero Lyapunov exponent Λ_0 on the amplitude A of the external harmonic signal is shown in Fig. 5. The behavior of the zero Lyapunov is shown both for the cases of absence (the numerically obtained data are shown by points ◇) and presence (●) of noise. The theoretical curves (32) are also shown in Fig. 5, with parameters and variables being selected as $f=0.156$, $a_1=7.5\times10^{-7}$, $a_2=1.01$, $\varepsilon_c=A_c=0.0238$, $\varepsilon=A$. To illustrate the accuracy of the analytical predictions the same points obtained numerically for $D=1.0$ as well as function (32) are shown in log-log scale both for the subcritical and supercritical regions (see frames in Fig. 5). Again, as well as in the case of the circle map, there is the excellent agreement between the theoretical predictions (32) and numerically obtained data in the whole range of the A-parameter values, except for a very tiny area $A\to A_c$ in the vicinity of the critical point A_c, where the theoretical predictions are not applicable.

Thus, the comparison of the theoretical predictions given in Sec. I and the results of numerical calculations of the circle map (23) and Van der Pol oscillator (28) proves the correctness of the developed theory.

III. PARTICULARITIES OF THE SYSTEM DYNAMICS CORRESPONDING TO THE NEGATIVENESS OF THE ZERO LYAPUNOV EXPONENT

Having deduced the expressions for the zero Lyapunov exponent and verified them numerically, let us consider now the particularities of the system dynamics (caused by the noise influence in the vicinity of the bifurcation point) corresponding to the negativeness of the zero Lyapunov exponent. For this purpose, the behavior of two unidirectionally coupled Rössler systems close to the phase synchronization boundary is considered. In this case there are both synchronization phenomenon and deterministic "noiselike" dynamics. The system under study is represented by a pair of unidirectionally coupled Rössler systems, whose equations read as

$$\begin{aligned} \dot{x}_d &= -\omega_d y_d - z_d, \\ \dot{y}_d &= \omega_d x_d + a y_d, \\ \dot{z}_d &= p + z_d(x_d - c), \\ \dot{x}_r &= -\omega_r y_r - z_r + \sigma(x_d - x_r), \\ \dot{y}_r &= \omega_r x_r + a y_r, \\ \dot{z}_r &= p + z_r(x_r - c), \end{aligned} \tag{33}$$

where (x_d,y_d,z_d) $[(x_r,y_r,z_r)]$ are the Cartesian coordinates of the drive (the response) oscillator, dots stand for temporal derivatives, and σ is a parameter ruling the coupling strength. The other control parameters of Eq. (33) have been set to $a=0.15$, $p=0.2$, $c=10.0$, by analogy with previous studies [9,30]. The ω_r parameter (representing the natural frequency of the response system) has been selected to be $\omega_r=0.95$; the analogous parameter for the drive system has been fixed as $\omega_d=0.93$. For such a choice of parameter values the systems (33) demonstrate the chaotic behavior, with both chaotic attractors of the drive and response systems being phase coherent. The instantaneous phases of the chaotic signals $\varphi(t)$ can be therefore introduced in a traditional way, as the rotation angle $\varphi_{d,r}=\arctan(y_{d,r}/x_{d,r})$ on the projection plane (x,y) of each system. The presence of the phase synchronization regime can be detected by means of monitoring the time evolution of the instantaneous phase difference, that has to fulfill the phase locking condition [22]

$$|\Delta\varphi(t)| = |\varphi_d(t) - \varphi_r(t)| < \text{const}. \tag{34}$$

Although the systems under study are completely deterministic, the chaotic dynamics of them may be considered as a random perturbation [18,26]. Stochastic models of the chaotic phase synchronization have been also considered in [31,32]. For example, in [18] the deformation of the scaling law for the mean length of the synchronized motion of

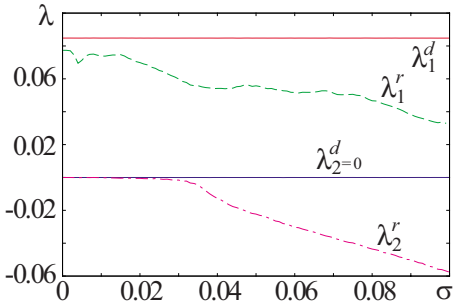

FIG. 6. (Color online) The dependence of the Lyapunov exponent spectrum on the parameter σ for two unidirectionally coupled Rössler systems (33). Conditional Lyapunov exponents are presented by dashed (λ_1^r) and dotted (λ_2^r) lines.

coupled Rössler oscillators in the vicinity of the synchronization regime had been explained, based on the random dynamics approach. Therefore, one can expect, that the revealed features in the behavior of the zero Lyapunov exponent taking place for the regular dynamics with noise may be also observed for the deterministic chaotic systems. The additional complexity in this case consists in the permanent chaotic perturbations in the system behavior, i.e., one cannot exclude the influence of "noise" on the system dynamics.

One more interesting point is the fact that the largest Lyapunov exponent of each chaotic oscillator (33) is positive due to the chaotic dynamics contrary to model systems (23) and (28) considered above, where the largest Lyapunov exponents were zero ones. So, the study of two coupled Rössler systems (33) allows us to give the answer to the question, whether the deduced analytical expressions (32) are correct in the case of chaotic dynamics or not.

The behavior of two unidirectionally coupled Rössler oscillators (33) is characterized by the Lyapunov exponent spectrum $\lambda_1 \geqslant \lambda_2 \geqslant \cdots \geqslant \lambda_6$. Due to the independence of the drive system dynamics on the behavior of the response one, the Lyapunov exponent spectrum may be divided into two parts: Lyapunov exponents of the drive system $\lambda_1^d \geqslant \lambda_2^d \geqslant \lambda_3^d$ and the conditional Lyapunov exponents $\lambda_1^r \geqslant \lambda_2^r \geqslant \lambda_3^r$ corresponding to the response oscillator. Figure 6 demonstrates the dependence of the fourth largest Lyapunov exponents (the other two Lyapunov exponents are about $\lambda_3^d \approx \lambda_3^r \approx -10.0$ and are not significant for our consideration) of coupled Rössler oscillators (33) on the coupling strength σ. Two of them, $\lambda_1^d > 0$ and $\lambda_2^d = 0$ correspond to the behavior of the drive system, therefore, they do not depend on σ. Two other quantities $\lambda_{1,2}^r$ are the conditional Lyapunov exponents. When the coupling parameter σ is equal to zero, $\lambda_1^r > 0$ and $\lambda_2^r = 0$. It is the second conditional Lyapunov exponent λ_2^r that attracts our interest being the subject of our study, i.e., $\Lambda_0 = \lambda_2^r$. With parameter σ increasing, on the one hand, the Lyapunov exponent under study $\Lambda_0 = \lambda_2^r$ becomes negative, and, on the other hand, the phase synchronization transition at $\sigma_{PS} \approx 0.039$ takes place.

More precisely, the zero Lyapunov exponent becomes different from zero as soon as the coupling between oscillators is switched on. This result has been reported for the first time in [16] for the Rössler oscillator driven by the external periodic force and is believed to be pretty general and to persist for the general case of two coupled chaotic oscillators [33]. For the considered two coupled Rössler oscillators (33) we have observed that in the vicinity of $\sigma_0 = 0$ (where the coupling between systems is just switched on), far away from the saddle-node bifurcation point, the quadratic dependence of the zero Lyapunov exponent on the coupling parameter is really observed, although the absolute value of the zero Lyapunov exponent is very small in this region, $|\Lambda_0| \sim 10^{-5} - 10^{-4}$. As the value of the coupling strength approaches the saddle-node bifurcation point, the zero Lyapunov exponent becomes negative sufficiently, with the theoretical predictions (32) being observed.

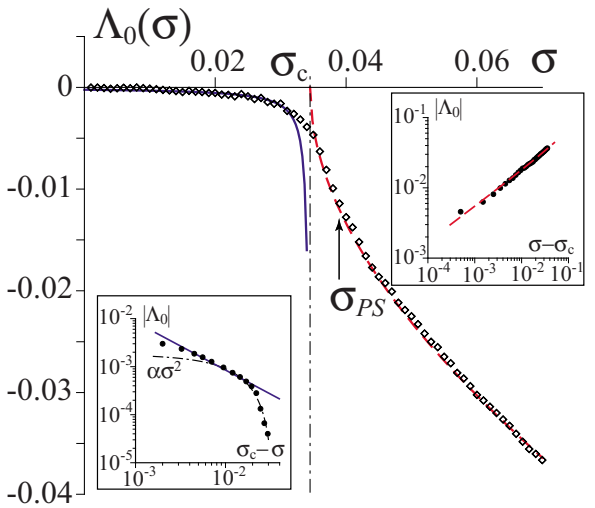

FIG. 7. (Color online) The dependence of the zero Lyapunov exponent Λ_0 on the control parameter σ in the vicinity of the boundary of phase synchronization for two unidirectionally coupled Rössler oscillators (33). The coupling strength value $\sigma_{PS} \approx 0.039$ corresponding to the onset of phase synchronization is shown by an arrow. The numerically calculated data are shown by points ◇. The analytical expressions for the zero Lyapunov exponent are shown by a solid line in the subcritical region and by a dashed line in the supercritical range of control parameter values. In the frames the same points obtained numerically as well as function (32) are shown in log-log scale both for the subcritical and supercritical regions. In the left-hand frame the quadratic function $\alpha\sigma^2$ is also shown by a dotted line, $\alpha = 1.51$.

The dependence of the Lyapunov exponent Λ_0 on the coupling strength σ near the boundary of the phase synchronization is shown in Fig. 7 in more detail. The theoretical curves (32) are also shown in Fig. 7, with parameters and variables being selected as $f = 0.148$, $a_1 = 8$, 5×10^{-6}, $a_2 = 1.16$, $\sigma_c = 0.0345$. As well as in the case considered in Sec. II B, in the frames in Fig. 7 the same dependence $\Lambda_0(\sigma)$ with its theoretical approximation are shown in log-log scale both for the subcritical and supercritical regions to illustrate the accuracy of the analytical predictions. In the left-hand frame corresponding to the subcritical region the quadratic function $\alpha\sigma^2$ deduced in [16] is also shown by a dotted line. Again, as well as in the cases of the model systems with noise added (circle map and Van der Pol oscillator), there is an excellent agreement between the theoretical predictions (32) and numerically obtained data. In the subcritical region one can see

that far away from the saddle-node bifurcation point, in the vicinity of $\sigma_0=0$, the dependence of the zero Lyapunov exponent on the coupling strength is described by the quadratic law $\alpha\sigma^2$, in the full agreement with the results of Ref. [16] and conditions (15) determining the range of the applicability of (32). When the coupling strength σ grows and approaches the saddle-node bifurcation point, the zero Lyapunov exponent deviates from the quadratic curve and its behavior is described by the theoretical prediction (32). So, we can conclude, that the theory developed for the systems with the random force may be applied successfully to the deterministic chaotic oscillators, such as Rössler systems.

The change of the sign of the Lyapunov exponents indicates generally a qualitative modification in the system dynamics. In some cases, the transition of the Lyapunov exponent to negative values is considered to be related to arising from the synchronous dynamics. Indeed, for the driven periodic oscillator the change of the sign of the zero Lyapunov exponent is connected with the onset of the synchronization regime. At the same time, for two coupled chaotic Rössler systems (33) the onset of the phase synchronization regime is observed when the zero Lyapunov exponent is essentially negative (Fig. 7, where the onset of the phase synchronization regime is shown with an arrow; see also [15]). Therefore, we can expect, that below the phase synchronization boundary some manifestations of the synchronism should be observed, although the phase synchronization regime does not take place yet.

The intermittent behavior may be treated as such kind of synchronism. Indeed, close to the threshold parameter values, for which the coupled systems show synchronized dynamics, it is observed that the desynchronization mechanism involves persistent intermittent time intervals during which the synchronized oscillations are interrupted by the nonsynchronous behavior. It is well known, that close to the phase synchronization boundary (for the small differences in the natural frequencies of the drive and response systems [45]) two types of intermittent behavior have been observed [23,34–36], namely the type-I intermittency and the superlong laminar behavior (so-called "eyelet intermittency" [37]). Below the boundary of the phase synchronization regime, the dynamics of the phase difference $\Delta\varphi(t)$ features time intervals of the phase synchronized motion (laminar phases) persistently and intermittently interrupted by sudden phase slips (turbulent phases) during which the value of $|\Delta\varphi(t)|$ jumps up by 2π.

Based on the consideration given above one can suppose that it is the presence of the synchronous phases that is connected with the negativeness of the zero Lyapunov exponent. To examine this assumption we have calculated the local (finite time) zero Lyapunov exponents [38,39] separately for the synchronous and asynchronous (phase slips) stages of chaotic motion.

The local Lyapunov exponents λ_l are calculated generally in fixed time intervals of length τ=const, and in this case one of the important characteristics is the distribution of the local Lyapunov exponents $N(\lambda_l)$ which is connected with the Lyapunov exponent value λ as

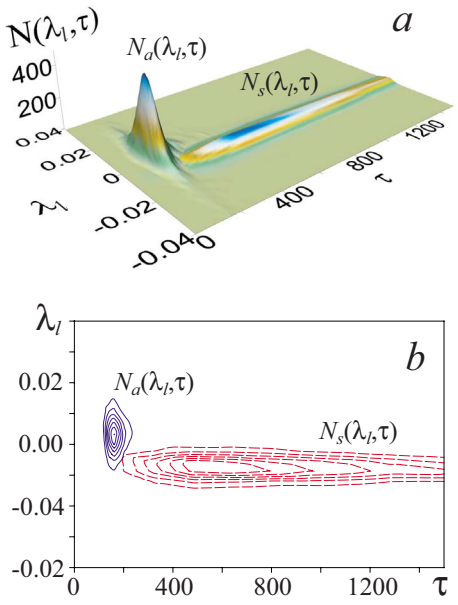

FIG. 8. (Color online) (a) The distributions of the local zero Lyapunov exponents obtained for the synchronous $[N_s(\lambda_l,\tau)]$ and asynchronous $[N_a(\lambda_l,\tau)]$ phases of chaotic motion of coupled Rössler oscillators (33) in the three-dimensional space (λ_l,τ,N). The coupling strength value $\sigma=0.034$, the zero Lyapunov exponent $\Lambda_0=-0037$. (b) The projection of distributions $N_s(\lambda_l,\tau)$ and $N_a(\lambda_l,\tau)$ on the plane (τ,λ_l).

$$\lambda=\frac{1}{N_0}\int_{-\infty}^{\infty}\lambda_l N(\lambda_l)d\lambda_l, \tag{35}$$

where $N_0=\int_{-\infty}^{\infty}N(\lambda_l)d\lambda_l$. In our study the local Lyapunov exponents are used to characterize the system dynamics in the synchronous and asynchronous stages, therefore, each local Lyapunov exponent is calculated in its own time interval τ corresponding to the particular phase, laminar or turbulent. Since the length τ of each of the laminar and turbulent phases is different, one must consider the distribution $N(\lambda_l,\tau)$ instead of $N(\lambda_l)$. Correspondingly, Eq. (35) should be replaced by

$$\lambda=\frac{\int_{-\infty}^{\infty}d\lambda_l\int_0^{\infty}\lambda_l\tau N(\lambda_l,\tau)d\tau}{\int_{-\infty}^{\infty}d\lambda_l\int_0^{\infty}\tau N(\lambda_l,\tau)d\tau}. \tag{36}$$

Since in our study the local zero Lyapunov exponents are considered for the laminar and turbulent phases separately, one obtains two distributions, $N_s(\lambda_l,\tau)$ and $N_a(\lambda_l,\tau)$, corresponding to the synchronous and asynchronous stages of chaotic motion, respectively. Obviously, the zero Lyapunov exponent Λ_0 is connected with these distributions as

$$\Lambda_0=\frac{\int_{-\infty}^{\infty}d\lambda_l\int_0^{\infty}\lambda_l\tau[N_s(\lambda_l,\tau)+N_a(\lambda_l,\tau)]d\tau}{\int_{-\infty}^{\infty}d\lambda_l\int_0^{\infty}\tau[N_s(\lambda_l,\tau)+N_a(\lambda_l,\tau)]d\tau}. \tag{37}$$

The distributions of the local zero Lyapunov exponents $N_s(\lambda_l,\tau)$ and $N_a(\lambda_l,\tau)$ calculated for the synchronous and asynchronous stages of dynamics of two coupled Rössler systems, respectively, are shown in Fig. 8. One can easily see, that the local zero Lyapunov exponents corresponding to the time intervals of synchronous motion are located in the

negative region of the values, while the analogous local zero Lyapunov exponents calculated for the phase slips (asynchronous stages of dynamics of coupled oscillators) are allocated in the vicinity of zero.

So, we conclude that the negativeness of the zero Lyapunov exponent is a manifestation of the presence of intervals in the time series where the synchronous behavior takes place. They are the phase of the synchronous motions that are responsible for the negativeness of the zero Lyapunov exponent values. At the same time, despite the fact, that the zero Lyapunov exponent is negative, there is no complete synchronous regime and the stages of the synchronous motion are interrupted by the phase slips. Thus, the negativeness of the zero Lyapunov exponent does not mean necessarily the existence of the phase synchronization regime, and, therefore, one must use this criterion carefully.

CONCLUSIONS

In the present paper the behavior of the zero Lyapunov exponent in the vicinity of the saddle-node bifurcation point has been considered. The laws for the dependence of this Lyapunov exponent on the control parameter both above and below the bifurcation point have been deduced analytically, with excellent agreement between the theoretical predictions and the data obtained by means of numerical calculations being observed (except for the very tiny range of the extremely small values of the control parameter ε, where, in full agreement with the developed theory, the analytical formulas diverge from the true values of Lyapunov exponent). Above the bifurcation point (i.e., in the supercritical region) the noise has practically no effect on the zero Lyapunov exponent, and its value Λ_0 coincides with the value of the corresponding Lyapunov exponent λ_0 characterizing the dynamics of a system without noise. As far as the subcritical region is concerned, noise turns the zero Lyapunov exponent Λ_0 into the negative values. The negativeness of the zero Lyapunov exponent is the manifestation of the presence of time intervals where the synchronous behavior takes place, although there is no complete regime of phase synchronization. Since the developed theory is applicable both to the systems with the random force and to the deterministic chaotic oscillators, we expect that the very same mechanism can be observed in many other relevant circumstances where the level of natural noise is sufficient, e.g. in the physiological [40–42] or physical systems [23].

ACKNOWLEDGMENTS

We thank the referees for valuable comments and remarks that allowed us to improve our paper. This work was partly supported by U.S. Civilian Research and Development Foundation for the Independent States of the Former Soviet Union (CRDF, Grant No. REC-006), Russian Foundation of Basic Research (Contracts No. 07-02-00044 and No. 08-02-00102), by the Supporting program of leading Russian scientific schools (Contract No. NSh-355.2008.2), and by the "Dynasty" Foundation. A.E.H. also acknowledges support from the President Program, Grant No. MD-1884.2007.2.

[1] K. Thamilmaran, D. V. Senthilkumar, A. Venkatesan, and M. Lakshmanan, Phys. Rev. E **74**, 036205 (2006).
[2] T. E. Karakasidis, A. Fragkou, and A. Liakopoulos, Phys. Rev. E **76**, 021120 (2007).
[3] W. M. Macek and S. Redaelli, Phys. Rev. E **62**, 6496 (2000).
[4] R. Porcher and G. Thomas, Phys. Rev. E **64**, 010902(R) (2001).
[5] R. M. Dünki, Phys. Rev. E **62**, 6505 (2000).
[6] S. P. Kuznetsov and D. I. Trubetskov, Radiophys. Quantum Electron. **47**, 341 (2004).
[7] S. P. Kuznetsov, Phys. Rev. Lett. **95**, 144101 (2005).
[8] K. Pyragas, Phys. Rev. E **54**, R4508 (1996).
[9] A. E. Hramov and A. A. Koronovskii, Phys. Rev. E **71**, 067201 (2005).
[10] D. S. Goldobin and A. Pikovsky, Phys. Rev. E **71**, 045201(R) (2005).
[11] D. S. Goldobin and A. Pikovsky, Physica A **351**, 126 (2005).
[12] A. E. Hramov, A. A. Koronovskii, and O. I. Moskalenko, Phys. Lett. A **354**, 423 (2006).
[13] M. G. Rosenblum, A. S. Pikovsky, and J. Kurths, Phys. Rev. Lett. **78**, 4193 (1997).
[14] G. V. Osipov, B. Hu, C. T. Zhou, M. V. Ivanchenko, and J. Kurths, Phys. Rev. Lett. **91**, 024101 (2003).
[15] A. E. Hramov, A. A. Koronovskii, and M. K. Kurovskaya, Phys. Rev. E **75**, 036205 (2007a).
[16] A. Politi, F. Ginelli, S. Yanchuk, and Y. Maistrenko, Physica D **224**, 90 (2006).
[17] A. E. Hramov, A. A. Koronovskii, and P. V. Popov, Phys. Rev. E **77**, 036215 (2008).
[18] W.-H. Kye and C.-M. Kim, Phys. Rev. E **62**, 6304 (2000).
[19] W.-H. Kye, S. Rim, C.-M. Kim, J.-H. Lee, J.-W. Ryu, B.-S. Yeom, and Y.-J. Park, Phys. Rev. E **68**, 036203 (2003).
[20] A. E. Hramov, A. A. Koronovskii, M. K. Kurovskaya, A. A. Ovchinnikov, and S. Boccaletti, Phys. Rev. E **76**, 026206 (2007).
[21] A. A. Koronovskii and A. E. Hramov, Eur. Phys. J. B **62**, 447 (2008).
[22] S. Boccaletti, J. Kurths, G. V. Osipov, D. L. Valladares, and C. T. Zhou, Phys. Rep. **366**, 1 (2002).
[23] S. Boccaletti, E. Allaria, R. Meucci, and F. T. Arecchi, Phys. Rev. Lett. **89**, 194101 (2002).
[24] A. S. Pikovsky, M. G. Rosenblum, and J. Kurths, Int. J. Bifurcation Chaos Appl. Sci. Eng. **10**, 2291 (2000).
[25] A. E. Hramov, A. A. Koronovskii, M. K. Kurovskaya, and S. Boccaletti, Phys. Rev. Lett. **97**, 114101 (2006b).
[26] A. S. Pikovsky, M. G. Rosenblum, G. V. Osipov, and J. Kurths, Physica D **104**, 219 (1997a).
[27] Y. Pomeau and P. Manneville, Commun. Math. Phys. **74**, 189 (1980).
[28] P. Manneville and Y. Pomeau, Physica D **1**, 167 (1980).

[29] P. Bergé, Y. Pomeau, and C. Vidal, *L'Ordre Dans Le Chaos* (Hermann, Paris, 1988).
[30] A. E. Hramov, A. A. Koronovskii, and O. I. Moskalenko, Europhys. Lett. **72**, 901 (2005).
[31] T. Yamada, T. Horita, K. Ouchi, and H. Fujisaka, Prog. Theor. Phys. **116**, 819 (2006).
[32] T. Horita, K. Ouchi, T. Yamada, and H. Fujisaka, Prog. Theor. Phys. **119**, 223 (2008).
[33] O. V. Popovych, Y. L. Maistrenko, and P. A. Tass, Phys. Rev. E **71**, 065201(R) (2005).
[34] A. S. Pikovsky, M. Zaks, M. G. Rosenblum, G. V. Osipov, and J. Kurths, Chaos **7**, 680 (1997).
[35] K. J. Lee, Y. Kwak, and T. K. Lim, Phys. Rev. Lett. **81**, 321 (1998).
[36] E. Rosa, E. Ott, and M. H. Hess, Phys. Rev. Lett. **80**, 1642 (1998).
[37] A. S. Pikovsky, G. V. Osipov, M. G. Rosenblum, M. Zaks, and J. Kurths, Phys. Rev. Lett. **79**, 47 (1997).
[38] A. Prasad and R. Ramaswamy, Phys. Rev. E **60**, 2761 (1999).
[39] R. Zillmer and A. S. Pikovsky, Phys. Rev. E **67**, 061117 (2003).
[40] A. E. Hramov, A. A. Koronovskii, V. I. Ponomarenko, and M. D. Prokhorov, Phys. Rev. E **73**, 026208 (2006).
[41] A. E. Hramov, A. A. Koronovskii, I. S. Midzyanovskaya, E. Sitnikova, and C. M. Rijn, Chaos **16**, 043111 (2006).
[42] A. E. Hramov, A. A. Koronovskii, V. I. Ponomarenko, and M. D. Prokhorov, Phys. Rev. E **75**, 056207 (2007).
[43] T. Horita, T. Yamada, and H. Fujisaka, Prog. Theor. Phys. Suppl. **161**, 199 (2006).
[44] Note, if the noise has a bounded amplitude, a sharp bifurcation phenomenon could be observed, see, e.g., [43].
[45] For the large differences in the natural frequencies the ring intermittency [25] takes place.